

## Grinding of Arc-Sprayed Tungsten Carbide Coatings on Machining Centers - Process Configuration and Simulation

D. Biermann<sup>1, a</sup>, T. Mohn<sup>1, a</sup>, H. Blum<sup>2, b</sup>, H. Kleemann<sup>2, b</sup>

<sup>1</sup>Institute of Machining Technology, Baroper Straße 301, 44227 Dortmund, Germany

<sup>2</sup>Chair of Scientific Computing, Vogelpothsweg 87, 44227 Dortmund, Germany

<sup>a</sup>{biermann;mohn}@isf.de, <sup>b</sup>{heribert.blum;heiko.kleemann}@mathematik.tu-dortmund.de

**Keywords:** Grinding, Coatings, Surface Engineering, Simulation, FEA

### Abstract

This paper describes the special demands placed on the grinding of arc-sprayed WC-Fe coatings on a conventional machining center. Basic process configuration, experimental results, measurement methods and an approach for a hybrid simulation system are presented.

### Introduction

The reduction of energy consumption in cars is one of the major aims of current developments in automotive industry. Forming of high-tensile steel-sheets is one major technology to obtain weight reduction in automotive applications. The higher resistance against deformation that these materials possess provides the desired stability of the auto body in crash situations but also leads to higher mechanical and tribological loads on the forming tools during the production process [1]. Thermal sprayed coatings provide a possible solution for reducing the abrasive wear in tribologically loaded environments [e.g. 2]. The aim of the collaborative research center SFB 708 at Technische Universität Dortmund (TU Dortmund) is to establish a working process chain that creates forming tools with an improved wear resistance by the thermal application of hard coatings. Achieving high surface quality and low form errors of the final sheets requires a mechanical machining of the coating. Grinding has been proven to be capable to create a higher wear resistance [e.g. 3] and to create compressive stresses into different thermal sprayed surfaces [4, 5]. This paper describes the fundamental investigations on grinding of a thermal sprayed WC-Fe coating that were carried out by face grinding processes. A coupled simulation system for this grinding process is under development to meet the necessity for a simulation of the process chain milling-coating-grinding - forming.

### Experimental Setup

To provide the geometrical flexibility to transfer the results to grinding of free-formed surfaces with small concave curvatures, the investigations were carried out on a common five-axis machining center “Deckel Maho DMU50 eVolution”, using small mounted points ( $D \leq 15$  mm) as grinding tools. The machining center does not provide special equipment for grinding processes, such as a high frequency spindle or dressing equipment. The maximum revolution speed of the spindle is 18,000 RPM. These basic conditions caused the necessity to develop a grinding process for thermal sprayed coatings with very low cutting speeds ( $v_{c, \max} = 10$  m/s) and to integrate a suitable dressing process into the machine. The setup is shown in Fig. 1. The dressing spindle was mounted on a precisely machined holding plate. Afterwards this assembly was measured in a 3D-coordinate measuring machine “ZEISS Prismo-Vast”. The data was used to calculate the position of the dressing wheel in order to compensate for mounting errors by transforming the coordinate system into the position and rotation of the dressing spindle during the dressing process. The direction and speed of the dressing wheel rotation could be set using a control panel for a separate frequency converter. All dressing processes in the investigations were performed with rotating diamond dressing wheels. A three component dynamometer was installed to measure the process forces that occur.

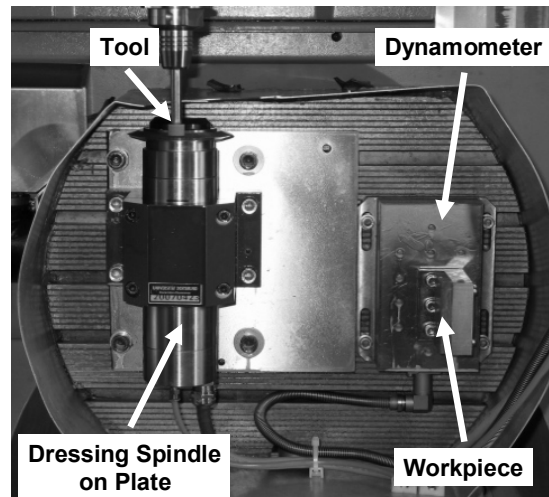


Figure 1: Experimental setup

The surface qualities resulting from the grinding processes were measured with a confocal 3D-Microscope “NanoFocus  $\mu$ surf” and a tactile sensor “Hommel T8000”. The macroscopic shape of the tools was studied using a “Zoller smartCheck” tool presetting and measuring machine. A scanning electron microscope “Philips XL 40 ESEM” was used to qualitatively analyze the grinding layers of the mounted points and the impact of the processes on the single grains. The material machined in this study was a tungsten carbide coating with iron bonding that was applied onto C45 steel workpieces (10 mm x 50 mm x 70 mm) by an arc spraying process at the Institute of Material Engineering (LWT) at Technische Universität Dortmund. According to the manufacturer’s information the porosity is less than 10 %. Further information on the material and the spraying processes is given in [2, 6]. The coating is composed of an iron matrix, 50 % tungsten carbide and small percentages of chrome, silicon and carbon with a hardness of 58 HRC-60 HRC [7].

### Tool Selection

It was necessary to use superabrasive cutting materials (diamond or cBN) because of the high amount of tungsten carbide in this coating. The selection of a tool concept for the grinding of the thermal sprayed coatings described was performed in two steps. Electroplated grinding tools were used to perform the selection of an appropriate grinding material. The high grain protrusion and the very low amount of bonding material (except of the identical nickel-plating) permitted the comparison of diamond and cBN grain as cutting materials, with a minimum influence of the bonding system. Afterwards, a comparison of different bonding systems (electroplating, vitrified and resin bonding) for the selected grain type took place. A DACE [8] based design of 40 experiments was performed for every tool system. All samples had been pre-machined on a surface grinding machine “Geibel & Hotz FS 635-Z CNC” to guarantee constant depths of cut for the following experiments.

The parameters that were varied in the plane grinding process on the machining center were the cutting speed  $v_c$ , feed speed  $v_f$ , depth of cut  $a_e$ , the process kinematics (up-/downgrinding) and grain size. The 1A1W-tools were of cylindrical shape. The processes were performed with no line feed. The poor surface qualities generated in these basic studies resulted from the process kinematics which reproduced the active profile of the grinding tools with high grain protrusion on the surface. Furthermore, the porosity of the thermal sprayed coating led to extreme peaks in the surface profiles which did not result from the grinding process (see “Surface Measurement”). As shown for the downgrinding with an average grainsize of  $d_g = 91 \mu\text{m}$  in Fig. 2, the use of cBN grain had no negative effect on the surface quality of the ground coating. The investigation of single grain wear using scanning electron microscopy showed no significant differences for diamond and cBN grain for when grinding with electroplated bonding [9]. CBN-based grinding tools can be flexibly shape-dressed with a diamond form roll inside the machining center which has the advantage of assuring the accurate profile of the tool for NC-shape grinding processes. This advantage and the

comparable grinding performance of the cBN and the diamond grain led to the selection of cBN as cutting material for the following processes.

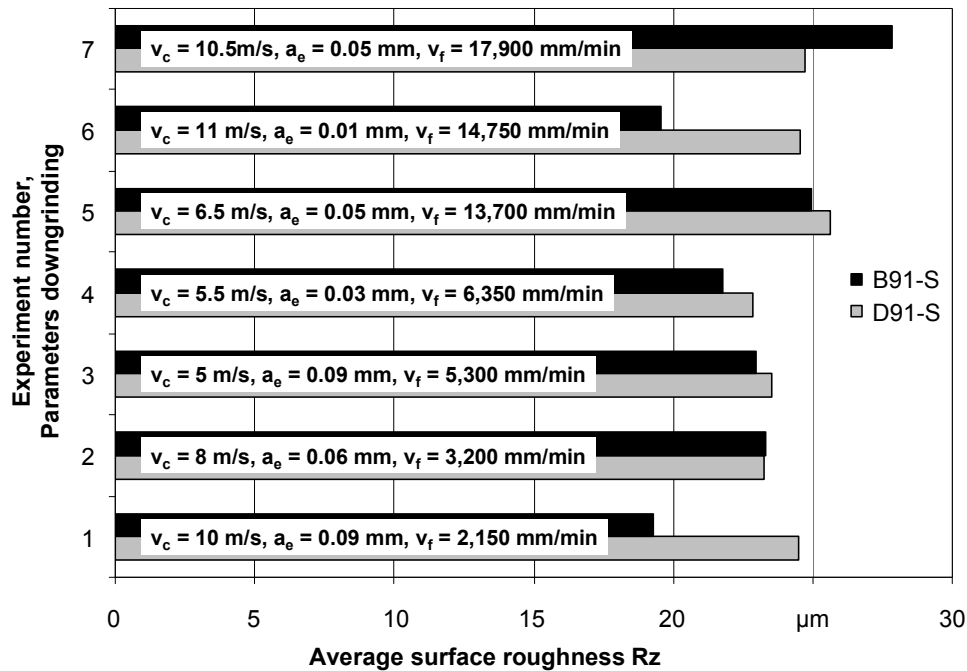


Figure 2: Surface roughness after face grinding with electroplated CBN and diamond tools

The dressing process for the vitrified bonded cBN tools was performed with a speed ratio of  $q = 0.7$ , a dressing infeed of  $a_{ed} = 10 \mu\text{m}$  and a total infeed of  $a_{ed,tot} = 200 \mu\text{m}$ . The dressing process showed no abnormalities, such as noise or macroscopic breakouts from the tool or the dressing wheel. The scanning electron micrographs showed a well-prepared tool surface with free grains, sharp edges and bonding support in cutting speed direction, as seen in Fig. 3.

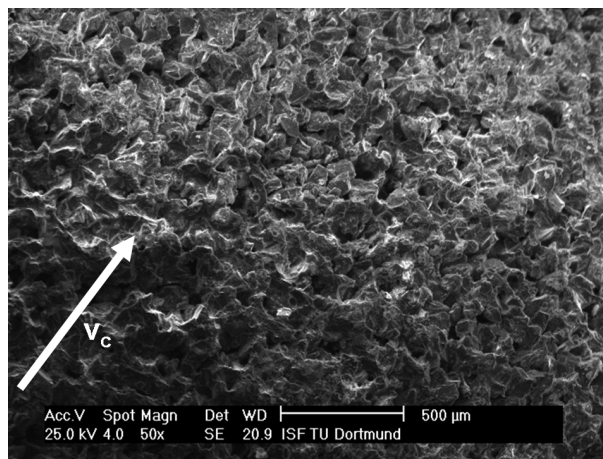


Figure 3: Grinding tool 1A1W-15-10-B91-V after dressing

The roundness and diameter of the vitrified bond tools were measured after the first and the last dressing process of each tool with a “Zoller smartCheck” tool presetting and measuring machine. These values corresponded to the nominal values within  $\pm 5 \mu\text{m}$ . The dressing process for the resin bond mounted points, which was performed with the same parameters as for the vitrified bond tools, was characterized by loud noise and vibration. The result of the dressing process was insufficient as it led to a visible waviness on the grinding tool and plastic deformation of the bonding layer. As a result of this waviness on the tool, the grinding process that was performed after sharpening the tool with a corundum block was characterized by extreme noise. The Fourier

analysis of the process forces during the grinding process revealed a dominant frequency peak of the vibration at the rotation speed of the tool at 425 Hz which can be interpreted as a result of an inefficient tool preparation as well as an extreme self-induced vibration at one higher frequency of 556 Hz. A visual and microscopic inspection of the diamond dressing wheel revealed many macroscopic breakouts from the metal bond diamond layer. The major damage of the dressing tool by the resin bond mounted point was the reason for selecting the vitrified bond cBN tools for further investigations.

### Surface Measurement and Influence of the Pores on the Measured Roughness

According to [3] the machining of thermal sprayed coatings, even with low porosity, leads to surface defects resulting from the uncovering of the pores in the material. A parallel optimization of the spraying parameters at the LWT allowed reducing the porosity of the coatings for the following grinding operations to less than 2 % by using a secondary gas stream [2, 6]. However the remaining porosity of the thermal sprayed coatings still results in high deviation of the  $R_z$  and  $R_a$  values that are measured on the ground surfaces. Depending on the pores in the profile section chosen for measurement, the standard deviation of the average roughness  $R_z$  was up to 14  $\mu\text{m}$  (or 97% deviation of the absolute values) on one workpiece after four tactile measurements with a measuring length of  $L = 4.8 \text{ mm}$  and a cut off of  $L_c = 0.8 \text{ mm}$ . Fig. 4 shows an example of the high influence of the pores and the selected profile section on the  $R_z$  value for one optical measurement of a ground coating. The workpiece was machined with a 1A1W-15-10-B126-V mounted point by pendulum grinding. The depth of cut was set at  $a_e = 0.04 \text{ mm}$ , the width of cut at  $a_p = 3.25 \text{ mm}$ . The cutting speed was kept constant at  $v_c = 10 \text{ m/s}$ , the feed speed at  $v_f = 600 \text{ mm/min}$  and the surface was sparked out three times. The direction of the profile sections was chosen at perpendicular to the grinding direction. As shown in Fig. 4 the extreme peaks in the roughness profile that lead to high values and deviation of the measured surface roughness can directly be related to the pores on the surface in each profile section.

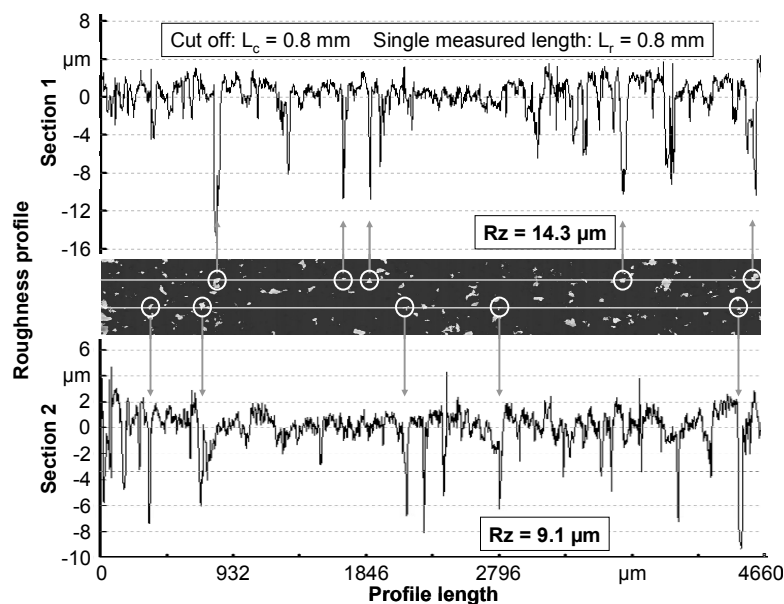


Figure 4: Influence of profile section and pores on the measured  $R_z$  value

To improve the comparability of the grinding processes the influence of the pores on the  $R_z$  and  $R_a$  values had to be reduced. Therefore it was necessary to process the measured data in a special way. The data from the optical 3D microscope had been analysed by use of the software tool “winSAM” that was developed at the Chair of Manufacturing Technology of the University of Erlangen. The tool was used to mark all pores below a certain material fraction as outliers and to get corrected values for  $R_a$  and  $R_z$ . After removing the pores from the profile measurement all 490 to 500 profile sections in each measuring field were analysed to calculate the average values. The boundary value

of the material fraction was kept constant for the different surfaces that were compared with each other. The material fraction has to be chosen on a level below the ground surface layer to allow to remove only pores without influencing the machined surface. The  $R_z$  values calculated by this method are marked as  $R_z'_{xx\%}$  in the following. The index  $xx\%$  stands for the boundary material fraction value. The effect of the different measurement methods on the stability index  $R^2$  of a quadric regression for the  $R_z$  values for surfaces resulting from the progression of tool wear in face grinding is illustrated in Fig. 5. It can be seen that this method leads to a higher quality of the average roughness model. The same effect on the regression models was seen when varying the feed angle (Fig.6) as well as other process parameters.

### Influence of the Microscopic Tool Wear on the Surface Quality

Fig. 5 illustrates the decreasing surface quality for higher stock removals that was caused by tool wear. The tool (1A1W-15-10-B91-V) was utilized in an upgrinding process with a cutting speed of  $v_c = 10$  m/s, a depth of cut of  $a_e = 60$   $\mu\text{m}$ , a feed speed of  $v_f = 1000$  mm/min and no line feed. The necessity for frequent dressing of the grinding tool is given by a decreasing surface quality with increasing stock removal. The experiment was repeated using tools with average grain sizes of  $d_{kg} = 126$   $\mu\text{m}$  and  $d_{kg} = 181$   $\mu\text{m}$  showing a similar behaviour. An examination of the tools used with scanning electron microscopy revealed microscopic wear mechanisms that were clearly dominated by failure of the vitrified bonding, such as grain breakouts and loss of bonding bridges (Fig. 5, right).

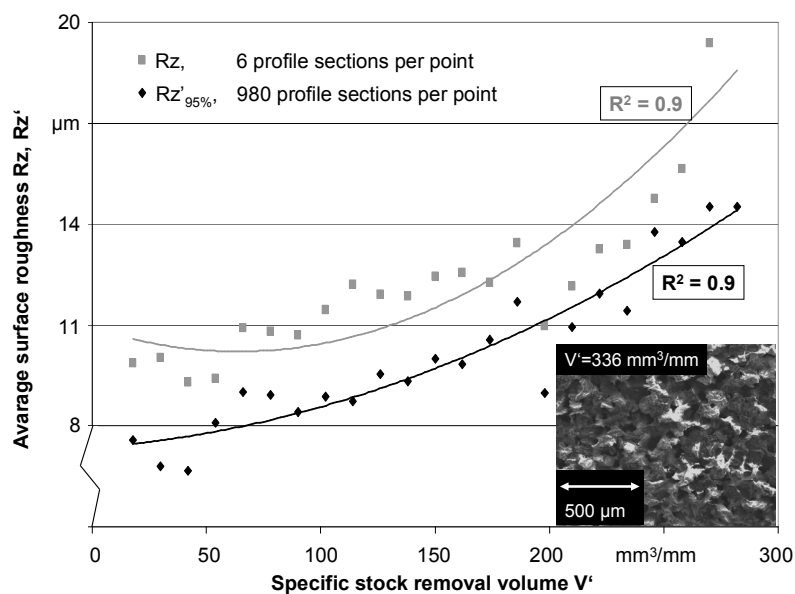


**Figure 5:** Development of surface roughness, improved measurement method and worn grinding layer

### Process Optimization

Based on the results of the face grinding processes, a pendulum grinding process with low feed speed and low depth of cut was the basis for surface quality optimization. A larger overlap of the single grain paths during the process caused by large feed angles and small line feeds might have the potential to minimize the resulting roughness. The grinding processes were performed with a 1A1W-15-10-B126-V tool that had been dressed before each experiment. Cutting speed was constantly set at  $v_c = 10$  m/s. The feed speed was kept constant at  $v_f = 600$  mm/min, the depth of cut at  $a_e = 0.04$  mm and the total depth of cut at  $a_{e,tot} = 0.08$  mm. To optimize the final quality, the surface was sparked out two times after each process. All samples were examined using confocal 3D microscopy. The values shown in Fig. 6 were averaged of 494 profile cross sections. The figure shows that by varying the feed angle  $\phi$  and the width of cut  $a_p$  (line feed) a satisfactory surface quality can be achieved, even at the low cutting speeds typical for grinding with small mounted points on machining centers.

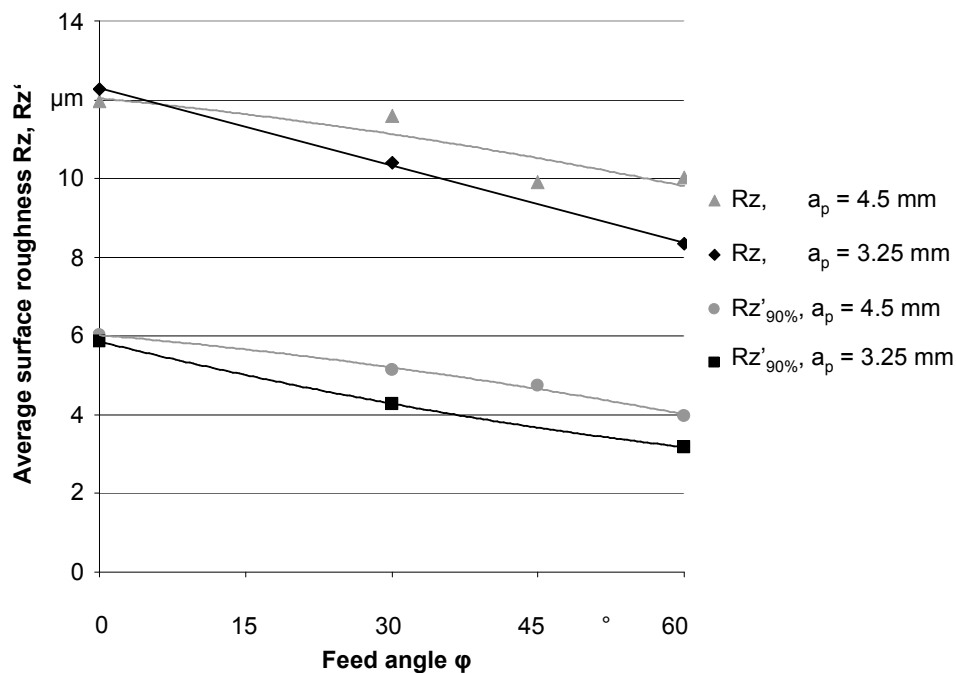


Figure 6: Influence of feed angle and width of cut on surface quality

### Simulation

The complete process chain for the production of the forming tool is simulated in the SFB 708 to avoid form errors of the tool and iterative rework. Due to the coating a postprocessing of the forming tool is very restricted, thus the form errors will be minimized by an optimization of the simulated process chain. The simulation of the grinding process will also be used to verify the process strategies and NC-data for shape grinding. Coupled geometric-kinematical and FEA-models can be used to analyse the dynamics of geometrically complex grinding processes [10, 11]. Therefore a geometric-kinematical simulation of the process will be coupled with an FE-analysis, to cover dynamical effects and process forces. This FE-simulation uses a coupled dynamic contact problem in 3D to predict the deformation and the contact forces of the grinding tool and the workpiece. Due to the changing contact situation one cannot expect that the finite element meshes fit in the contact zone. This is covered by applying a mixed variational problem formulation, which allows the use of nonmatching meshes. The mathematical details of the finite element analysis can be found in [12].

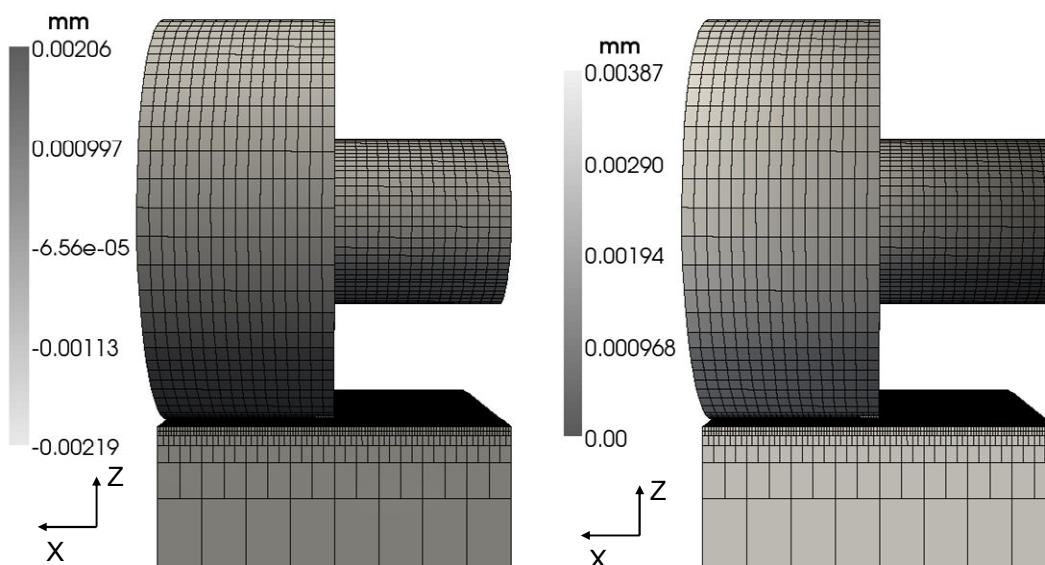


Figure 7: Deformation of grinding tool in x (left) and z (right) direction

In Fig. 7 the resulting contact situation for a depth of cut of  $a_e = 40 \mu\text{m}$  in z-direction is illustrated. As expected the main deformation is found in the shank of the grinding tool: The vertical deformation of the shank (right) leads to a maximal deformation in z-direction of  $u_z = 38 \mu\text{m}$  of the grinding tool, whereas the maximal deformation of the workpiece is only about  $u_z = 2 \mu\text{m}$ . The resulting deformation in horizontal direction of the grinding tool (left) leads to a new coupling situation between grinding tool and workpiece, which has to be taken into account in order to achieve an appropriate approximation of the forces in the contact area. Though the deformation of the workpiece is essentially smaller than the deformation of the grinding tool, the workpiece should not be considered rigid, as the coating of the workpiece is the subject of interest and the computed inner stresses will also be used to predict potential failure of the coating due to the grinding process. The deformation of the grinding tool in x-direction cannot be covered by a 2D simulation so that the full 3D model promises a better prediction of the grinding process. To illustrate the benefit of the grinding tool deformation, the resulting equivalent von Mises stress of the workpiece is shown in Fig. 8 on the right under assumption of a rigid tool and on the left using the coupled model. The stresses resulting on the rigid tool are significantly higher than those computed by the coupled model and also the contact zone is larger and this would lead to false removal and failure predictions.

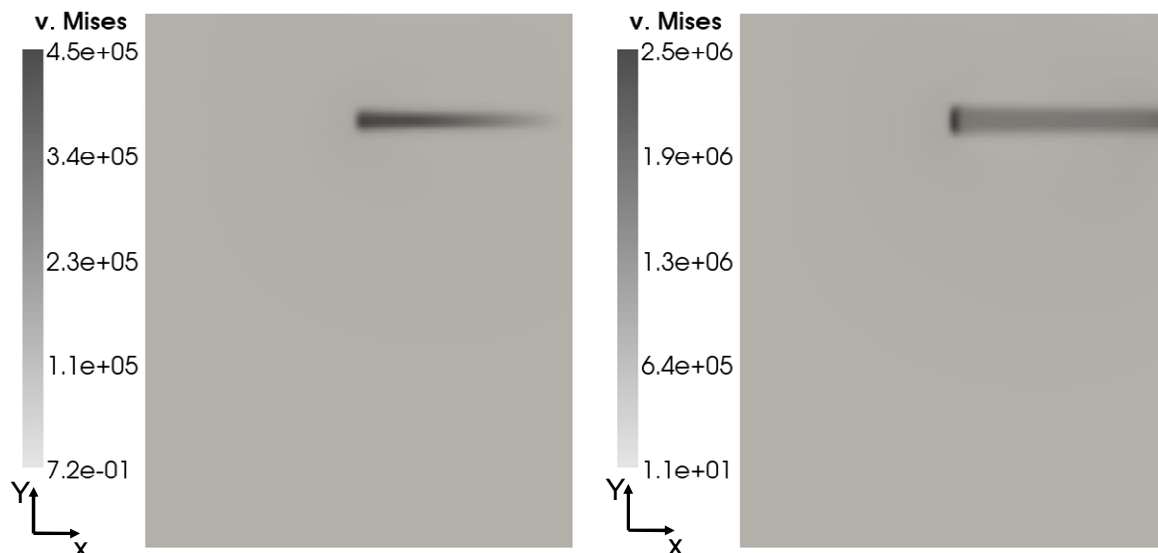


Figure 8: eq. v. Mises stress of the workpiece with rigid tool (right) and deformable tool (left)

## Conclusions

The grinding of arc-sprayed WC-Fe coatings on machining centers is dominated by certain restrictions resulting from the low cutting speed, the dressing system and the morphology of the coating. Vitrified bond cBN mounted points were shown to be suitable tools for these processes. To obtain a satisfactory surface quality the use of spark out strokes and low feed speeds are necessary along with a frequent dressing of the grinding tool. Further improvements can be achieved by high feed angles and low widths of cut that lead to higher overlaps of the single grain paths on the ground surfaces. Resin bond tools can not be dressed with the chosen parameters and dressing system. Therefore further investigations concerning grinding on machining centers should include the variation of the dressing tool and parameters for shape dressing of vitrified bond mounted points. The measurements for the surface roughness are dominated by the influence of the pores that are not a result of the grinding process but of the morphology of the coating. An optimized measurement method for minimizing these influences and to allow a better comparison of the grinding processes has been introduced. Further investigations on 5-axis grinding will be based on these results so as to create low-friction sheet forming tools with proper shape accuracy and high resistance against tribological load. The hybrid simulation system introduced will be the basis to compensate the accruing form errors that may occur as a result of the mechanical loads during these complex grinding processes.

---

**References:**

- [1] Klocke F.; Timmer, A.: Werkzeuge aus Keramik: ein riesiges Potenzial. Tiefziehen Blech InForm \* (2008) No. 6, P 49-52, ISSN 1616-3362
- [2] Tillmann, W. et.al.: Desirability-Based Multi-Criteria Optimization of HVOF Spray Experiments to Manufacture Fine Structured Wear-Resistant 75Cr3C2-25(NiCr20) Coatings. Journal of Thermal Spray Technology, published Online, 03 September 2009
- [3] Edinger, M.: Untersuchung zur spanenden Endbearbeitung und zum Funktionsverhalten von thermisch gespritzten Verschleißschutzschichten. Dissertation University of Kaiserslautern 1996
- [4] Murthy, J et. al.: Effect of grinding on the erosion behavior of a WC-Co-Cr coating deposited by HVOF and detonation gun spray processes. Wear, Vol. 249, 2001, 7, S. 592-600
- [5] Deng, Z. et. al.: Experimental Investigations of Surface Residual Stresses in the As-Sprayed and Ground Nanostructured WC/12Co Coatings. Key Engineering Materials, Vols. 359-360 2008, S. 229-233
- [6] Tillmann, W.; et. al.: Thermally sprayed wear-protective cermet coatings for forming tools; Proc. of 4th International Conference on Spray Deposition and Melt Atomization (SDMA); Bremen, Germany, September 7-9, 2009
- [7] Durum Verschleißschutz GmbH: „Produktdatenblatt Durmat AS-850“, [http://www.durmat.com/PDFFiles/Datenblaetter\\_de/Therm\\_spritzdraechte/DURMAT%20AS-850.pdf](http://www.durmat.com/PDFFiles/Datenblaetter_de/Therm_spritzdraechte/DURMAT%20AS-850.pdf), January 7th, 2010
- [8] Sacks, J.et.al.: Design and Analysis of Computer Experiments. Statistical Science 4 (1989), P. 409-435
- [9] Blum, H.; Biermann, D.; Kleemann, H.; Mohn, T.: Simulationsgestütztes Schleifen frei geformter, beschichteter Oberflächen mit Hilfe angepasster Schleifstifte. In: SFB 708 - 2. öffentliches Kolloquium., 21.11. 2008, ISBN: 978-3-89957-072-4, P. 155-165
- [10] Denkena, B. et. al.: Modeling and Simulation of the Process Machine Interaction during Tool Grinding Processes. (2007) In: Proceedings of the 10th CIRP International Workshop on Modeling of Machining Operations, August 27-28, 2007, Reggio Calabria, Italy, P. 391-398, 2007
- [11] Biermann, D.; Mohn, T.: A Geometric-Kinematical Approach for the Simulation of Complex Grinding Processes. In: Proceedings of the 6th CIRP International Conference on Intelligent Computation in Manufacturing Engineering (CIRP ICME '08), 2008, Naples, Italy, Teti, R. (Publisher), ISBN: 978-88-900948-7-3, P. 401-408
- [12] Blum, H.; Kleemann, H., Rademacher, A., Schröder A.: On solving frictional contact problems part III: Unilateral contact. tech. rep., Fakultät für Mathematik, TU Dortmund, (2009). Ergebnisberichte des Instituts für Angewandte Mathematik.